Front. Phys. 13(4), 137307 (2018)
https://doi.org/10.1007/s11467-018-0797-8

RESEARCH ARTICLE

Electronic and optical properties of single-layer MoS_2

Hai-Ming Dong[1], San-Dong Guo[1,†], Yi-Feng Duan[1], Fei Huang[2], Wen Xu[3,4,‡], Jin Zhang[4,#]

[1] *School of Physical Science and Technology, China University of Mining and Technology, Xuzhou 221116, China*
[2] *Low Carbon Energy Institute, China University of Mining and Technology, Xuzhou 221116, China*
[3] *Key Laboratory of Materials Physics, Institute of Solid State Physics, Chinese Academy of Sciences, Hefei 230031, China*
[4] *Department of Physics, Yunnan University, Kunming 650091, China*
Corresponding authors. E-mail: [†] *guosd@cumt.edu.cn,* [‡] *wenxu_issp@aliyun.com,* [#] *zhangjin96@aliyun.com*
Received December 7, 2017; accepted March 14, 2018

The electronic structures of a MoS_2 monolayer are investigated with the all-electron first principle calculations based on the density functional theory (DFT) and the spin-orbital couplings (SOCs). Our results show that the monolayer MoS_2 is a direct band gap semiconductor with a band gap of 1.8 eV. The SOCs and d-electrons in Mo play a very significant role in deciding its electronic and optical properties. Moreover, electronic elementary excitations are studied theoretically within the diagrammatic self-consistent field theory. Under random phase approximation, it shows that two branches of plasmon modes can be achieved via the conduction-band transitions due to the SOCs, which are different from the plasmons in a two-dimensional electron gas and graphene owing to the quasi-linear energy dispersion in single-layer MoS_2. Moreover, the strong optical absorption up to 10^5 cm^{-1} and two optical absorption edges I and II can be observed. This study is relevant to the applications of monolayer MoS_2 as an advanced photoelectronic device.

Keywords MoS_2, electronic and optical properties

PACS numbers 73.22.-f, 73.61.-r, 78.66.-w

Frontiers of Physics

1 Introduction

In 2004, Novoselov and Geim extracted graphene, which is an allotrope of carbon in the form of a two-dimensional (2D), atomic-scale, hexagonal lattice. Graphene has drawn an enormous attention throughout the world owing to its unusual and exceptional properties. However, graphene is a zero-gap semiconductor and cannot support a cut-off current in devices, which greatly limits its applications as a novel optoelectronic device. In recent years, scientists have achieved and investigated 2D, graphene-like, electronic materials such as WS_2, MoS_2, and black phosphorus [1]. The bulk MoS_2, an indirect-gap semiconductor with a band gap of 1.29 eV, is built up of van der Waals bonded S-Mo-S units. In contrast to gapless graphene, a monolayer MoS_2 is a direct band-gap semiconductor with a 1.8 eV energy gap, making it an excellent candidate for the development of field-effect transistors, photodetectors, and electroluminescent devices. Single-layer MoS_2 exhibits a room-temperature high current on/off ratio and mobility [2]. It shows that forming MoS_2 is an important step towards the realization of advanced electronics and low-standby-power integrated circuits. In addition, researchers in Switzerland have developed a series of electronic devices with excellent performance based on single-layer MoS_2 [3].

In addition, monolayer MoS_2 displays distinct optical properties. Yin *et al.* fabricated a new phototransistor based on the single-layer MoS_2, which displays a better photo-responsivity and prompts photo-switching in contrast to the graphene-based optoelectronic device [4]. It has been shown that the monolayer MoS_2 can emit photons strongly, with a luminescence quantum efficiency of more than 10^4 compared with the bulk material [5]. Single-layer MoS_2 with an energy bandgap of 1.8 eV has been proposed as top-gate phototransistors with green-light detection capability [6]. Through ab initio numerical simulations and experimental microphotoluminescence, Wang and others have demonstrated that monolayer MoS_2 reveals near-perfect valley-selective circular dichroism due to its bulk symmetry and is very much conducive to optoelectronic valley polarization [7]. It has been demonstrated that the single-layer MoS_2

field-effect transistors can be used as integrated small-signal analog amplifiers [8]. The two photoluminescence (PL) peaks are observed at low temperatures [9]. These important findings indicate that MoS_2 systems can be potentially applied as novel nano-optoelectronic devices. Similar to WS_2, WSe_2, $MoSe_2$, and TiS_2, MoS_2 is one of the typical layered chalcogenides of transition-metals, in which the electrons in the d-orbitals (d-electrons) play a very important role. Moreover, the spin-orbit couplings (SOCs) and the quantum confinement effects (QCE) become even more distinct and significant for electrons in d-orbitals [10]. New physical phenomena and effects can be achieved using such 2D layered systems, considering the QCE and the interactions between the d-electrons. The electronic and optical properties are determined by electronic structures. Furthermore, the electronic collective excitations, called plasmons, reflect the most basic photoelectronic properties of materials. Motivated by the important experimental findings, in order to understand the electronic properties of the monolayer MoS_2 at a deeper level, we attempted to investigate the electronic structures, electronic and optical properties of a MoS_2 monolayer, and studied the elementary electronic excitations under random phase approximation in detail.

2 Theoretical approaches

2.1 Electronic structures

In this work, we considered a monolayer MoS_2 in the xy-plane on top of a dielectric wafer. In order to investigate on the electronic properties of such a system, the energy band structures of monolayer MoS_2 are obtained within density functional theory as implemented in the WIEN2k package [11]. The local-density approximation (LDA) is adopted to describe the exchange-correlation potential, and the SOCs is included by the second variation method [12]. Moreover, the total density of states (DOS) and partial density of states (PDOS) of monolayer MoS_2 are obtained from the first-principles calculations in order to study its electronic properties at a deeper level. Monolayer MoS_2 is composed of one layer of molybdenum atoms sandwiched between two layers of sulfur atoms with a total thickness of 0.65 Å. The bulk unit cell of MoS_2 with the space group $P6_3/mmc$ includes 6 atoms, namely 2 Mo and 4 S atoms.

2.2 Energy eigenvalues and wave functions in low energy region

Based on the first principles calculations, a $\boldsymbol{k}\cdot\boldsymbol{p}$ Hamiltonian for monolayer MoS_2 is

$$H = at(\tau k_x\hat{\sigma}_x + k_y\hat{\sigma}_y) + \frac{\Delta}{2}\hat{\sigma}_z + \gamma\tau\frac{\hat{\sigma}_z - 1}{2}\hat{S}_z. \tag{1}$$

Here, $\hat{\sigma}$ represent the Pauli matrices and $\hat{S}_z$ is the spin matrix for the z component. τ refers to the valley index. In this work, we only study the electronic and optical properties of monolayer MoS_2 at the K-point in low energy, without spin-valley and trigonal warping effects. The effective Hamiltonian for a carrier (an electron or a hole) in the monolayer MoS_2 at the K-point in low energy region can then be written as 2×2 simplified Hamiltonian, which is

$$H(\boldsymbol{k}) = \begin{bmatrix} \Delta/2 & at(k_x - \mathrm{i}k_y) \\ at(k_x + \mathrm{i}k_y) & -\Delta/2 + s\gamma \end{bmatrix}, \tag{2}$$

where $\boldsymbol{k}$ represents the wave-vector for a carrier in the x-y plane. $s = \pm 1$ refer to spin up and spin down, respectively. The lattice parameter is $a = 3.193$ Å and the nearest-neighbor hopping parameter is $t = 1.1$ eV. The spin-orbit coupling parameter equals $\gamma = 75$ meV and Δ is the direct band gap energy with a value 1.8 eV for MoS_2. Earlier, the complete Hamiltonian for the group-VI dichalcogenides was proposed and developed by Xiao [10]. The corresponding Schödinger equations for the system can be solved analytically. The eigenvalues are given by

$$E^s_\lambda(\boldsymbol{k}) = s\gamma/2 + \lambda\sqrt{\chi^2k^2 + (\Delta - s\gamma)^2/4}, \tag{3}$$

where $\lambda = +1$ for the conduction bands and $\lambda = -1$ for the valence bands in monolayer MoS_2 and $\chi = at$. The corresponding eigenfunction for carriers near K-point is

$$\psi^s_\lambda(\boldsymbol{r}) = N^s_\lambda(\boldsymbol{k})[\chi k\mathrm{e}^{-\mathrm{i}\phi}/B^s_\lambda(\boldsymbol{k}), 1]\mathrm{e}^{\boldsymbol{k}\cdot r}, \tag{4}$$

where $k = \sqrt{k_x^2 + k_y^2}$, $\boldsymbol{r} = (x, y)$, $B^s_\lambda(\boldsymbol{k}) = E^s_\lambda(\boldsymbol{k}) - \Delta/2$, and the normalization factor $N^s_\lambda(\boldsymbol{k}) = |B^s_\lambda(\boldsymbol{k})|/[(B^s_\lambda(\boldsymbol{k}))^2 + \chi^2k^2]^{1/2}$.

2.3 DOS and Fermi energy at the K-point in low energy region

The free-particle Green's function for a carrier is

$$G_{\lambda\boldsymbol{k}}(E) = [E - E_\lambda(\boldsymbol{k}) + \mathrm{i}\delta]^{-1}, \tag{5}$$

with E being the carrier energy. Thus, the DOS for the system is determined by the imaginary part of the Green's function, which reads

$$D^s_\lambda(E) = \sum_{\boldsymbol{k}}\delta[E - E_\lambda(\boldsymbol{k})] = \frac{|2E - s\gamma|}{2\pi\chi^2}\Theta(\lambda E). \tag{6}$$

With the carrier DOS, the Fermi energy E_F of the system can be determined by using the carrier number conservation constraint. Using the Fermi–Dirac function as statistic energy distribution for carriers, we have

$$n^s_\lambda = \int_0^\infty D^s_\lambda(E)f(E)\mathrm{d}E, \tag{7}$$

where n_+ (n_-) is the electron (hole) density for different spin subbands. Our expression of DOS shows that SOCs play a key role near Fermi energy in deciding the electronic properties of monolayer MoS_2.

2.4 Plasmons

In this work, we study the elementary electronic excitation induced by electron-electron (e-e) in MoS_2 systems. Therefore, we consider n-type MoS_2 samples with an electron density n_e in conduction bands and with a hole density $n_h = 0$ in its fully-occupied valence bands. In a diagrammatic self-consistent theory, for the e-e scatterings, the dynamical dielectric function $\epsilon(q,\omega)$ can be written as

$$\epsilon(q,\omega) = 1 - (v_q/2)\sum_{\boldsymbol{k}}(1+\lambda'\lambda A_{\boldsymbol{k}q})\Pi(\boldsymbol{k},\boldsymbol{q};\omega), \tag{8}$$

where $\boldsymbol{q} = (q_x, q_y)$ is the change of the carrier wavevector during an e-e scattering event, $v_q = 2\pi e^2/(\epsilon_\infty q)$ is the 2D Fourier transform of the e-e Coulomb interactions, $A_{\boldsymbol{k}q} = (k + q\cos\theta)/|\boldsymbol{k}+\boldsymbol{q}|$, and θ is the angle between $\boldsymbol{k}$ and $\boldsymbol{q}$.

$$\Pi_{\lambda'\lambda}(\boldsymbol{k},\boldsymbol{q};\omega) = \frac{f[E_{\lambda'}(\boldsymbol{k}+\boldsymbol{q})] - f[E_\lambda(\boldsymbol{k})]}{\hbar\omega + E_{\lambda'}(\boldsymbol{k}+\boldsymbol{q}) - E_\lambda(\boldsymbol{k}) + \mathrm{i}\delta}$$

is the pair bubble or density-density correlation function in the absence of e-e interactions. Here we assume that the momentum-distribution function for a carrier can be described by a Fermi-distribution function $f[x]$.

Due to Landau damping, the plasmon is damped and decayed into the electron-hole pairs, in which the imaginary part of the dielectric function $\mathrm{Im}\epsilon(q,\omega) \neq 0$. In general, the plasmon modes are strongly damped for large q, and the plasmons in the valence bands are also damped, which cannot be observed in experiments [13]. Hence, the umdamped plasmon excitations can be achieved via intra-band transitions in the conduction bands. The modes of plasmons in presence of electric fields are determined by $\mathrm{Re}|\epsilon| \to 0$. In the long-wavelength ($q \to 0$) and low temperature ($T \to 0$) limit, we have the collective-mode frequencies under random phase approximation, which are,

$$\omega_1 = \frac{e\chi}{2\hbar}\left(\frac{n_+}{\pi\epsilon_\infty}\right)^{1/2}\frac{q^{1/2}}{[16\pi\chi^2 n_+ + (\Delta-\gamma)^2]^{1/4}}, \tag{9}$$

induced by the electron transitions in spin up subbands ($s = +1$) of the conduction band, and

$$\omega_2 = \frac{e\chi}{2\hbar}\left(\frac{n_-}{\pi\epsilon_\infty}\right)^{1/2}\frac{q^{1/2}}{[16\pi\chi^2 n_- + (\Delta+\gamma)^2]^{1/4}}, \tag{10}$$

induced by the electron transitions in spin down subbands ($s = -1$) of the conduction band. It is noted that the plasmon modes we obtained were very different from the previously reported theoretical results [14]. In this work, we obtained the analytical expressions of plasmons for the first time based on the simplified Hamiltonian with SOCs. In addition, we achieved the same plasmon modes for the other valley index near K′-point, because the energy dispersions are very similar for different valleys.

2.5 Optical properties

With the help of the complex dielectric function ϵ including the real and imaginary parts, we were able to investigate and discuss the optical properties of electron systems by DFT. By using $\epsilon = \epsilon_1 - \mathrm{i}\epsilon_2$, we can calculate the optical constants, which can be measured experimentally, as shown below:

$$n = \left(\frac{\sqrt{\epsilon_1^2+\epsilon_2^2}+\epsilon_1}{2}\right)^{1/2}, \tag{11}$$

and

$$\kappa = \left(\frac{\sqrt{\epsilon_1^2+\epsilon_2^2}-\epsilon_1}{2}\right)^{1/2}, \tag{12}$$

where n is the refractive index and κ is the coefficient of light extinction. Furthermore, the optical conductivity and absorption coefficient are respectively given by

$$\sigma = \omega\epsilon_2/(4\pi), \tag{13}$$

and

$$\alpha = 4\pi\sigma/(nc), \tag{14}$$

where c is the speed of light in vacuum.

3 Numerical results and discussion

The electronic structures evaluated using the first-principles calculations are shown in Fig. 1; the inset shows the energy bands near Fermi surface in the low energy region. It is clearly seen that monolayer MoS_2 is a direct-gap semiconductor with a band gap of $\Delta = 1.8$ eV. As is well known, the generalized gradient approximation (GGA) or LDA can be used to estimate the gaps of the semiconductors. However, for monolayer MoS_2, the LDA gap of 1.86 eV is very close to the experimental value of 1.9 eV [15]. The GGA and experimental gaps of monolayer $MoSe_2$ (1.44 eV and 1.55 eV) and WSe_2 (1.56 eV and 1.64 eV) are very close in value in Ref. [16]. The HSE or GW gaps of MoS_2, $MoSe_2$, and WSe_2 are further away from the experimental values than those

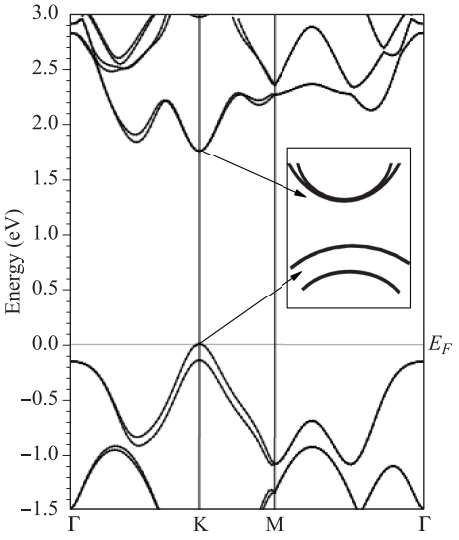

Fig. 1 The electronic structure of monolayer MoS_2 as evaluated from the first-principles calculations. E_F is Fermi energy. Inset shows the energy bands near Fermi surface in the low energy region.

of GGA or LDA [17]. Therefore, LDA or GGA may be suitable for these 2D materials for calculating the energy band gap. It shows that the SOCs plays a very significant role in the electronic structures, especially in the low energy region. As shown in the inset of Fig. 1, the SOCs leads to the energy band splitting (spin splitting). Both the subbands of energy bands on the bottom of the conduction bands and on the top of the valence bands, respectively, were discovered. The electronic and optical properties were determined by the four subbands of energy bands near Fermi surface. It is clear that our results obtained by using DFT in low energy are in very good agreement with the electronic structures from the $k \cdot p$ theory [18]. Figure 2, shows the total DOS and PDOS of monolayer MoS_2, evaluated using DFT calculations; these were used to understand the electronic structures of single-layer MoS_2 at a deeper level. It was found that all the DOS were mainly due to the contribution of Mo atom d-orbital electrons near Fermi energy, which result in obvious SOCs. Therefore, the d-orbital electrons in Mo played a fundamental role in deciding the electronic properties of monolayer MoS_2. These results are in agreement with the experimental findings [2, 7]. Moreover, our calculations are consistent with the previously reported theoretical results [19].

Figure 3 shows plasmon frequency ω_1 via the same spin subband transition ($s = +1$) in conduction bands for different electron densities. It shows that plasmon mode ω_1 via the same subband transition ($s = +1$), $\omega_1 \sim q^{1/2}$, is acoustic-like and depends strongly on q. The frequency of the plasmon increases with an increasing electron densities. It shows that the plasmon frequency can be effectively controlled by tuning the electron density. Figure 4 shows the plasmon dispersion ω_2 in spin down ($s = -1$) subband transitions for different electron densities. Similar to ω_1, ω_2 is also acoustic-like and depends strongly on q and electron density. However, the plasmon modes $\omega_1 \propto (\Delta - \gamma)^{-1/2}$ and $\omega_2 \propto (\Delta + \gamma)^{-1/2}$, are different because of the SOCs and as is evident, $\omega_1 > \omega_2$. With $\gamma = 75$ meV and $\gamma \ll \Delta$, we obtain $\delta = (\omega_1 - \omega_2) \sim \gamma \cdot q^{1/2} \cdot n_e^{-3/4}$, which shows that the difference δ between both the plasmon modes enlarges with increasing q or decreasing n_e. As a result, we can obtain two branches or colors of plasmon excitations at the same time by controlling the electron density in single-layer MoS_2.

In conventional semiconductors based on 2D electron gas systems (C2DEG), the plasmon frequency is $\omega_p = (2\pi e^2 n_e q/m_e^*)^{1/2}$ where m_e^* is the electron effective mass, while the plasmon frequency in graphene is $\omega_p' = [2e^2 E_F q/(\hbar^2 \epsilon_\infty)]^{1/2}$ where ϵ_∞ is the high-frequency dielectric constant [13]. It is obvious that the plasmon excitations in single-layer MoS_2 are different from plasmon excitations in C2DEG and graphene. The reason behind it is that the quasi-linear energy dispersions of single-layer MoS_2 are different from the parabolic en-

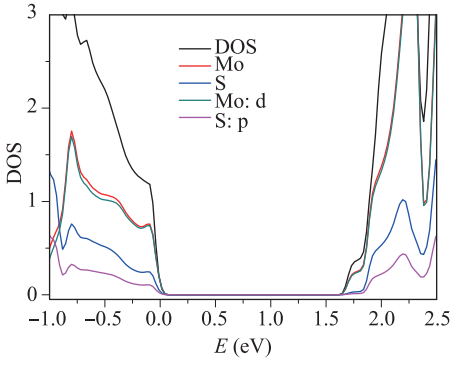

Fig. 2 The total density of states and partial density of states of monolayer MoS_2 evaluated from the first-principles calculations

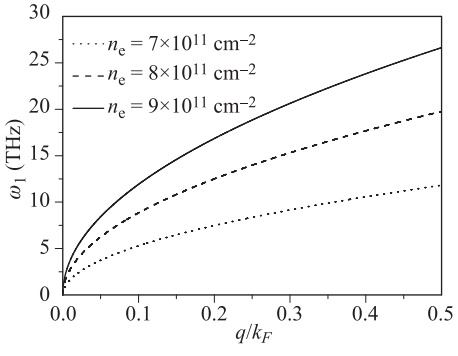

Fig. 3 Plasmon frequency ω_1 in spin up ($s = +1$) subband transitions for different electron densities.

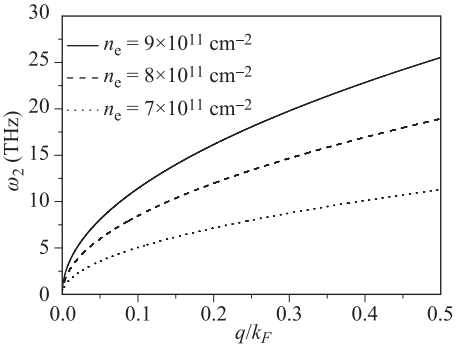

Fig. 4 Plasmon frequency ω_2 in spin down ($s = -1$) subband transitions for different electron densities.

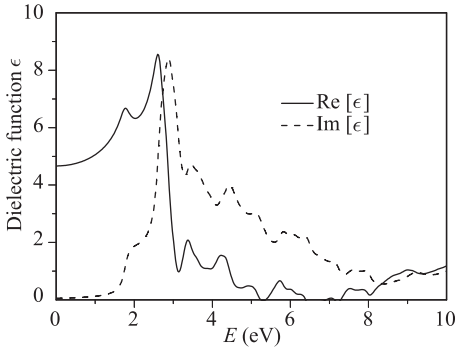

Fig. 5 The real and imaginary parts of the dielectric function ϵ as a function of photon energy E.

ergy dispersion in C2DEG and linear energy dispersion in graphene. Owing to the distinct SOCs, the plasmon excitations of a single-layer MoS_2 not only depend on q and electron density, but also on the band-gap Δ and the strength γ of the SOCs. It shows that the SOCs originating from the d-electrons in Mo has a very significant effect on the electronic and optical properties of single-layer MoS_2.

The real part, ϵ_1, and imaginary part, ϵ_2, of the complex dielectric function, ϵ, are shown in Fig. 5. The dielectric function ϵ indicates the micro response of materials to external fields. One can acquire the macroscopic physical quantities, such as optical absorption coefficient and refractive index using this function. A broadening that is used in these calculations, leads to a small number below the band gap. Figure 6 shows the optical absorption coefficient as a function of photon energy in monolayer MoS_2. A strong optical absorption can be observed with an optical absorption coefficient α of the order of 10^5 cm^{-1}. In addition, two the optical absorption edges I and II are observed indicating that two optical absorption channels can be achieved in such systems. The inset in Fig. 6 shows the two optical absorption channels. Due to the spin splitting from the SOCs, the valence band splits into the two subbands. The electrons in both the subbands absorb photons and transit into the conduction

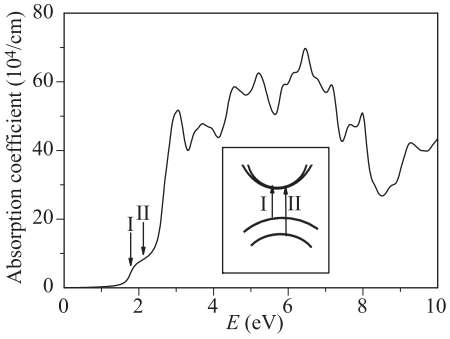

Fig. 6 The optical absorption coefficient, obtained from the dielectric function, as a function of photon energy E. Inset shows the optical absorption channels I and II.

band via the channels I and II. As a result, two optical absorption edges, I and II, can be found. These theoretical results are in line with the experimental results [5, 8, 9]. Finally, at the time of submission of our work, we noticed that the similar results had been published in which the same results by the first principles study have been reported [20].

4 Conclusion

It was found that monolayer MoS_2 is a direct-gap semiconductor with a band gap $\Delta = 1.8$ eV. The SOCs plays a very significant role in forming the electronic structures, especially in the low energy region. The total DOS are mainly due to the contribution of the Mo d-orbital electrons near Fermi energy, which results in obvious SOCs. These plasmon excitations were found to be different from those in C2DEG and graphene because of the quasi-linear energy dispersions in MoS_2. A strong optical absorption was observed and the optical absorption coefficient α was found to be of the order of 10^5 cm^{-1}. Moreover, two optical absorption channels were achieved in the system due to the spin splitting from the SOCs. Our theoretical findings have demonstrated that the single-layer MoS_2 can be used in designing novel optoelectronic nanodevices.

Acknowledgements This work was supported by the National Natural Science Foundation of China (Grant Nos. 11604380, 11774416 and 11574319), and the Provincial Natural Science Foundation of Jiangsu (Grant No. BK20151138).

References

1. A. H. Castro Neto and K. Novoselov, New directions in science and technology: Two-dimensional crystals, *Rep. Prog. Phys.* 74, 082501 (2011)

2. B. Radisavljevic, A. Radenovic, J. Brivio, V. Giacometti, and A. Kis, Single-layer MoS_2 transistors, *Nat. Nanotechnol.* 6(3), 147 (2011)
3. B. Radisavljevic, M. B. Whitwick, and A. Kis, Integrated circuits and logic operations based on single-layer MoS_2, *ACS Nano* 5(12), 9934 (2011)
4. Z. Y. Yin, H. Li, H. Li, L. Jiang, Y. M. Shi, Y. H. Sun, G. Lu, Q. Zhang, X. D. Chen, and H. Zhang, Single-layer MoS_2 phototransistors, *ACS Nano* 6(1), 74 (2012)
5. K. F. Mak, C. Lee, J. Hone, J. Shan, and T. F. Heinz, Atomically thin MoS_2: A new direct-gap semiconductor, *Phys. Rev. Lett.* 105, 136805 (2010)
6. H. S. Lee, S. W. Min, Y. G. Chang, M. K. Park, T. Nam, H. Kim, H. Kim Jae, and S. Ryu, MoS_2 nanosheet phototransistors with thickness-modulated optical energy gap, *Nano Lett.* 12(7), 3695 (2012)
7. T. Cao, G. Wang, W. P. Han, H. Q. Ye, C. Zhu, J. Shi, Q. Niu, P. Tan, E. Wang, B. Liu, and J. Feng, Valley-selective circular dichroism of monolayer molybdenum disulphide, *Nat. Commun.* 3(1), 887 (2012)
8. B. Radisavljevic, M. B. Whitwick, and A. Kis, Small-signal amplifier based on single-layer MoS_2, *Appl. Phys. Lett.* 101, 043103 (2012)
9. T. Korn, S. Heydrich, M. Hirmer, J. Schmutzler, and C. Schüller, Low-temperature photocarrier dynamics in monolayer MoS_2, *Appl. Phys. Lett.* 99(10), 102109 (2011)
10. D. Xiao, G. B. Liu, W. Feng, X. Xu, and W. Yao, Coupled spin and valley physics in monolayers of MoS_2 and other group-VI dichalcogenides, *Phys. Rev. Lett.* 108(19), 196802 (2012)
11. P. Blaha, K. Schwarz, G. K. H. Madsen, D. Kvasnicka, and J. Luitz, WIEN2k, An Augmented PlaneWave + Local Orbitals Program for Calculating Crystal Properties, Karlheinz Schwarz Technische University Wien, Austria, 2001
12. D. D. Koelling and B. N. Harmon, A technique for relativistic spin-polarised calculations, *J. Phys. C* 10(16), 3107 (1977)
13. H. M. Dong, L. L. Li, W. Y. Wang, S. H. Zhang, C. X. Zhao, and W. Xu, Terahertz plasmon and infrared coupled plasmon–phonon modes in graphene, *Physica E* 44(9), 1889 (2012)
14. A. Scholz, T. Stauber, and J. Schliemann, Plasmons and screening in a monolayer of MoS_2, *Phys. Rev. B* 88(3), 035135 (2013)
15. X. Li, J. T. Mullen, Z. Jin, K. M. Borysenko, M. Buongiorno Nardelli, and K. W. Kim, Intrinsic electrical transport properties of monolayer silicene and MoS_2 from first principles, *Phys. Rev. B* 87(11), 115418 (2013)
16. S. Kumar and U. Schwingenschlögl, Thermoelectric response of bulk and monolayer $MoSe_2$ and WSe_2, *Chem. Mater.* 27(4), 1278 (2015)
17. Y. Ding, Y. L. Wang, J. Ni, L. Shi, S. Q. Shi, and W. H. Tang, First principles study of structural, vibrational and electronic properties of graphene-like MX_2 (M=Mo, Nb, W, Ta; X=S, Se, Te) monolayers, *Physica B* 406(11), 2254 (2011)
18. A. Kormányos, V. Zólyomi, N. D. Drummond, P. Rakyta, G. Burkard, and V. I. Fal'ko, Monolayer MoS_2: Trigonal warping, the Γ valley, and spin-orbit coupling effects, *Phys. Rev. B* 88, 045416 (2013)
19. E. S. Kadantsev and P. Hawrylak, Electronic structure of a single MoS_2 monolayer, *Solid State Commun.* 152(10), 909 (2012)
20. Q. Luan, C. L. Yang, M. S. Wang, and X. G. Ma, First-principles study on the electronic and optical properties of WS_2 and MoS_2 monolayers, *Chin. J. Phys.* 55(5), 1930 (2017)